Histopathology and Clinical Implication of Treatment-related Image Changes After Surgical Resection of Brain Metastases Previously Treated with Gamma Knife Radiosurgery

Jeong-Hwa Kim
Samsung Medical Center
Jung-Il Lee (jilee@skku.edu)
Samsung Medical Center, Sungkyunkwan University School of Medicine https://orcid.org/0000-0001-8143-5513
Jung-Won Choi
Samsung Medical Center, Sungkyunkwan University School of Medicine
Doo-Sik Kong
Samsung Medical Center, Sungkyunkwan University School of Medicine
Ho-Jun Seol
Samsung Medical Center, Sungkyunkwan University School of Medicine
Do-Hyun Nam
Samsung Medical Center, Sungkyunkwan University School of Medicine

Research Article

Keywords: radiation necrosis, treatment-related image changes, brain metastasis, gamma knife radiosurgery

Posted Date: March 5th, 2021

DOI: https://doi.org/10.21203/rs.3.rs-265578/v1

Abstract

INTRODUCTION

The true pathology and clinical implication of treatment-related image changes (TRICs) after stereotactic radiosurgery (SRS) for brain metastases (BM) have not been established. This study compared the surgical pathology and outcomes of intracranial metastatic lesions featured as TRICs or progressive disease (PD) in advanced magnetic resonance imaging (MRI).

METHODS

A total of 86 patients who underwent surgical resection of brain metastases previously treated with gamma knife radiosurgery (GKS) from 2009 to 2019 were retrospectively reviewed and classified by MRI findings and histopathology.

RESULTS

Among 54 patients with TRICs in preoperative MRI, the histopathology of pure radiation necrosis (RN) was confirmed in 19 patients (TRIC-RN) and mixed or predominant viable tumor cells in 35 patients (TRIC-PD). Thirty-two patients diagnosed with PD exhibited the metastatic histology well correlated with imaging (PD-PD). The TRIC-PD group showed larger prescription isodose volume (9.4 cm^3) than the TRIC-RN (4.06 cm^3, p=0.014) group and shorter time interval from GKS to preoperative MRI diagnosis related to neurological deficits (median 4.07 months) than the PD-PD group (median 8.77 months, p=0.004). Significant differences in progression-free survival were confirmed among the three groups (p<0.001) but not between TRIC-RN and TRIC-PD (post hoc test, p=1.00), whereas no significant difference was observed in overall survival (p=0.067).

CONCLUSIONS

The brain metastatic lesions diagnosed as TRICs after GKS frequently contained viable tumor cells, while they exhibited the benign prognosis as RN after surgical resection. These findings suggest that TRICs on advanced MRI can serve as a prognostic factor, regardless of the histologic heterogeneity.

Introduction

Treatment-related image changes (TRICs) occur months to years after stereotactic radiosurgery (SRS), and the histology of TRICs is usually considered to be radiation necrosis (RN). Symptomatic focal brain necrosis developed in 2–10% of patients who underwent gamma knife radiosurgery (GKS) for brain metastases (BM)[1–3], and the overall risk of RN leading to permanent morbidity and additional surgical resections was reported as 4.7–7.0%[4–6].

Based on current imaging diagnoses, it is not easy to predict true pathology and clinical outcome of TRICs [7]. Differentiating them from progressive disease (PD) has been a challenge after stereotactic radiosurgery for brain metastasis, due to their similar magnetic resonance imaging (MRI) appearances with enlarged, heterogeneous rim enhancement in the T1-weighted sequence[8]. Discordance between radiologic and histologic diagnoses may lead to the misdiagnosis of local lesions and inadequate determination of the systemic treatment protocols[7, 9, 10].

To the best of our knowledge, there have been few reports about the true pathology of radiation-changed lesions. The study retrospectively analyzed the pathologic and clinical outcomes of TRICs and progressive disease (PD) in metastatic tumors that were surgically resected due to clinical worsening after SRS, therefore, aimed to elucidate the clinical implications of TRICs which are not always equivalent to RN.

Methods

Study cohort

Between April 2009 and May 2019, the medical records of 211 patients who underwent surgical resection after gamma knife radiosurgery for BMs at our institute were retrospectively reviewed.
Approval was obtained from the SMC Institutional Review Board.
Patients with GKS dosimetry reports, advanced MRI sequences to discriminate TRICs and PD, and sufficient clinical follow-ups using MRI for at least 6 months after surgery were included. We excluded patients with other surgical pathologies, acute intracranial hemorrhage or abscess, and preoperative GKS as adjuvant therapy. Patients who survived less than 6 months postoperatively were also excluded.

Radiosurgical treatment

Radiosurgery was performed with the Leksell Gamma Knife® Perfexion™ from 2009 to 2015 or the Leksell Gamma Knife® Icon™ (both Elekta AB, Stockholm, Sweden) from April 2016 onwards. The 1.0-mm slices of T1-weighted and 2.0-mm slices of T2-weighted fluid-attenuated inversion recovery (FLAIR) contrast-enhanced MR images were obtained and transferred to the Leksell GammaPlan Software version 11.1.1 (Elekta AB). The target volume was defined as the contrast-enhancing tumor volume, and the dosimetry planning was carried out in accordance with the RTOG (Radiation Therapy Oncology Group) 90 – 05 study guidelines[11, 12].

Imaging diagnosis with the advanced MRI protocols

The patients were clinically followed-up and evaluated with MRI every 2–3 months after radiosurgery. Each patient was scanned by 3-T MRI using the tumor protocol, including pre- and post-contrast 5-mm-thick axial spin echo T1-weighted image, 5-mm-thick axial fat-suppressed echo T2-weighted image, 5-mm-thick axial fluid attenuation inversion recovery (FLAIR), diffusion weighted image (DWI) which was performed with spin echo EPI using a b-value of 0 and 1000 s/mm^2 (TR/TE = 3000/80 ms, slice thickness 5¼ mm, interslice gap = 1.5 mm, and acquisition matrix = 128 × 128), dynamic susceptibility contrast (DSC)-PWI (TR/TE = 1720/35 ms, flip angle = 40°, slice thickness = 5 mm, interslice gap = 1.5 mm, acquisition matrix = 128 × 128, 50 volumes, and acquisition time = 1 min 30 s). The amount of contrast agent was 0.1 mmol/kg × 3cc/s with power injector (Dotarem [gadoterate meglumine]; Guerbet, Aulnay-sous-Bois, France) in DSC-MRI.

For post-GKS lesions that exhibited an increased extent of T1-enhancement with FLAIR hyperintensity in follow-up MRI, tumor progression was suspected if a solid enhancement pattern, relatively high cerebral blood volume (CBV), and more restricted diffusion were observed. TRICs were preferably diagnosed through a “soap bubble” or “Swiss cheese” sign of enhancement, low or constant CBV, and less restricted diffusion [7, 10, 13–15].

Indication for surgical resection and postoperative follow-up

After GKS, surgical resection was planned if neurological deficits or symptoms of increased intracranial pressure (IICP) presented in patients with Karnofsky performance scale (KPS) score of > 60, and more than 3 months of life expectancy. All outpatients were prescribed oral steroids, and intravenous steroids and mannitol were administered to patients readmitted for urgent surgery to control the IICP and relieve the neurological symptoms and signs related to the lesion mass effect. No patient was treated with bevacizumab for RN. Patients underwent routine outpatient follow-up 1 month after surgery and were further evaluated at 3-month intervals thereafter, with the data reported up to July 2020.

Statistical analysis

Patient demographics and clinical data were summarized using standard descriptive statistics and frequency tabulation. If statistically significant results indicated non-equal distribution, post hoc tests were used to identify the significant differences between the groups. Overall survival (OS) of patients was calculated from the time of resection until death or last follow-up. Progression-free survival (PFS) was defined as the time from the surgical resection to the diagnosis of local progression of the resected lesion. Survival probability was estimated using the Kaplan-Meier product-limit method.

Univariable and multivariable analyses were performed using a binary logistic regression model to identify the probability factors for local progression and survival.
Statistical significance was determined when the p-value was less than 0.05. SAS version 9.4 (SAS Institute, Cary, NC) was used for all statistical analyses.

Results

Patient classification

A total of 86 patients were included in the final analysis. Based on the radiological and surgical pathology, patients were classified into three groups (Fig. 1). For preoperative imaging, TRIC was diagnosed in 54 (62.7%) patients and PD in 32 (37.3%). Among the TRIC patients, the surgical pathology confirmed RN in only 19 of the 54 (35.2%) patients, whereas the other 35 (64.8%) patients revealed mixed (11 of 35, 31.5%) or pure metastatic (24 of 35, 68.5%) histology, represented as the TRIC-RN and TRIC-PD groups, respectively. The 32 cases of MRI-diagnosed tumor progression were all histopathologically confirmed as tumor progression and included in the PD-PD group.

Patient demographics and lesion characteristics

The preoperative patient characteristics and treatment parameters are shown in Table 1. The median age of the entire study population was 58 years (range: 40–81 years). Most metastatic lesions were located in the frontal (40, 46.5%) and parietal (22, 25.6%) regions with similar proportions in all three groups (p = 0.754). Sixteen patients underwent fractionated radiosurgery due to prolonged beam-on-time of more than 2 hours. There was a mean isodose of 24 Gy in three fractions for 14 patients, and 18 Gy in two fractions and 30 Gy in four fractions for one patient each.

Table 1
Patient demographics and treatment parameters

	Total (n = 86)	TRIC-RN (n = 19)	TRIC-PD (n = 35)	PD-PD (n = 32)	p-value
Median age, year (range)	58 (40 – 81)	57 (40–77)	58 (40–74)	58 (41–81)	0.943
Sex (%)	36 (41.9)	7 (36.8)	15 (42.9)	14 (43.8)	0.879
Male	50 (58.1)	12 (63.2)	20 (57.1)	18 (56.2)	
Female					
Primary malignancy (%)	57 (66.3)	14 (73.7)	27 (77.1)	16 (50.0)	0.169
Lung	15 (17.4)	2 (10.5)	5 (14.3)	8 (25.0)	
Breast	14 (16.3)	3 (15.8)	3 (8.6)	8 (25.0)	
Other §					
Prior GKS for target lesion (%)	28 (32.6)	12 (63.2)	9 (25.7)	7 (21.9)	0.005*
Yes	58 (67.4)	7 (36.8)	26 (74.3)	25 (78.1)	*-2.68 0.007†*
No					
Prior WBRT (%)	18 (20.9)	7 (36.8)	7 (20.0)	4 (12.5)	0.117
Yes	68 (79.1)	12 (63.2)	28 (80.0)	28 (87.5)	
No					
Location (%)	40 (46.5)	8 (42.1)	17 (48.6)	15 (46.9)	0.754
Frontal	22 (25.6)	6 (31.5)	10 (28.5)	6 (18.7)	
Parietal	5 (5.8)	1 (5.3)	1 (2.9)	3 (9.4)	
Temporal	7 (8.1)	1 (5.3)	2 (5.7)	4 (12.5)	
Occipital	11 (12.8)	2 (10.5)	5 (14.3)	4 (12.5)	
Cerebellum	1 (1.2)	1 (5.3)	0 (0)	0 (0)	
Other					
Median PIV, cm^3 (range)	6.41 (0.14 – 62.29)	4.06 (0.14 – 34.50)	9.40 (1.50 – 40.72)	6.80 (0.89 – 62.29)	0.014* *0.031¶*

*overall p-value

† z- and p-values of the Jonckheere-Terpstra test

¶ p-value of the post hoc test

§ renal cell cancer (3), colorectal cancer (4), melanoma (2), hepatocellular carcinoma (2), cholangiocarcinoma, endometrial carcinoma, thyroid cancer

GKS = gamma knife radiosurgery; PD = progressive disease; PIV = prescription isodose volume; RN = radiation necrosis; TRIC = treatment-related image change; WBRT = whole-brain radiation therapy.

	Total (n = 86)	TRIC-RN (n = 19)	TRIC-PD (n = 35)	PD-PD (n = 32)	p-value
Median prescription isodose, Gy (range)	18 (8 – 25)	18 (14 – 25)	18 (8 – 22)	17 (12 – 23)	0.605
Median time interval GKS to TRIC/PD, months (range)	6.07 (1.01 – 40.03)	5.43 (1.01 – 39.60)	4.07 (1.03 – 18.13)	8.77 (1.03 – 40.03)	0.004* *<0.001¶*
Primary malignancy control (%)	41 (47.7)	9 (47.4)	14 (40.0)	18 (56.3)	0.413
Controlled	45 (52.3)	10 (52.7)	21 (60.0)	14 (43.8)	
Uncontrolled					
*overall p-value					
† z- and p-values of the Jonckheere-Terpstra test					
¶ p-value of the post hoc test					
§ renal cell cancer (3), colorectal cancer (4), melanoma (2), hepatocellular carcinoma (2), cholangiocarcinoma, endometrial carcinoma, thyroid cancer					
GKS = gamma knife radiosurgery; PD = progressive disease; PIV = prescription isodose volume; RN = radiation necrosis; TRIC = treatment-related image change; WBRT = whole-brain radiation therapy.					

There were significant differences in GKS history among the three groups (p = 0.005). A much higher percentage of patients (63.1%) in the TRIC-RN group had a history of prior GKS, whereas 9 (25.7%) had it in the TRIC-PD group and 7 (21.6%) in the PD-PD group (Jonckheere-T□erpstra test=-2.68, p = 0.007). No significant difference was observed for history of whole brain radiation therapy.

The median prescription isodose volume (PIV) was 6.41 cm^3 (range: 0.14–62.29 cm^3). Statistical differences were observed among the median PIVs of the three groups (p = 0.014), and the median PIV of the TRIC-RN group (4.06 cm^3, range 0.14–34.50 cm^3) was smaller than that of the TRIC-PD group (9.40 cm^3, range 1.50–40.72 cm^3) in the post hoc test (p = 0.031). Radiation doses were prescribed to 50% isodose line in all patients with a median isodose of 18 Gy (range: 8–25 Gy).

The median time from the date of GKS to the imaging diagnosis was 6.07 months (range: 1.01–40.03 months). Upon post hoc analysis, the TRIC-PD group exhibited a shorter time to imaging diagnosis than the PD-PD group (4.07 months, [range: 1.03–18.13 months] vs. 8.77 months [range: 1.03–40.03 months], respectively; p < 0.001).

Surgical outcomes

After imaging diagnosis, 81 patients (94%) underwent surgical resection within 4 weeks, and the other 5 patients within 6 weeks. Preoperative neurological deficits were headache in 57 patients, motor weakness in 27, nausea and vomiting in 16, seizure in 13, and aphasia in 10. The median preoperative KPS score of the patients was 70 (range: 60–90). Total resection of the lesions was conducted in most of the patients to relieve the cerebral mass effect and promote better local control, except two patients of the PD-PD group underwent subtotal lesionectomy due to poorly demarcated tumor related to irradiation or adherence to an anatomically critical structure such as anterior clinoid process.

The median postoperative KPS score was 80 (range: 50–90), better than the preoperative KPS score in all three groups. The neurological deficits improved for most patients (66, 76.6%) but were sustained or worse after surgery in the other 20 (23.3%) patients (Table 2).

Table 2
Univariate and multivariate analyses for risk of death and tumor recurrence

		Overall survival				Progression-free survival			
		Univariate analysis		Multivariate analysis		Univariate analysis		Multivariate analysis	
Continuous data		HR (95% CI)	p-value	HR (95% CI)	p-value	HR (95% CI)	p-value	HR (95% CI)	p-value
Age, years		1.004 (0.974 – 1.035)	0.801	NA	-	1.023 (0.990 – 1.057)	0.154	NA	
PIV, mm^3		0.992 (0.967 – 1.017)	0.519	0.971 (0.944 – 1.000)	0.048	1.007 (0.981 – 1.032)	0.615	1.001 (0.973 – 1.031)	0.925
Prescription isodose, Gy		0.941 (0.852 – 1.040)	0.234	NA	-	0.887 (0.796 – 0.989)	0.030	0.912 (0.778 – 1.067)	0.250
Time interval GKS – TRIC or PD, months		0.966 (0.930 – 1.003)	0.069	0.961 (0.921 – 1.003)	0.071	0.999 (0.968 – 1.031)	0.957	0.990 (0.950 – 1.032)	0.643
Categorical data									
TRIC-RN		1	0.757*	1	0.055*	1	0.0002*	1	0.002*
TRIC-PD		2.313 (1.008 – 5.308)	0.048	3.342 (1.153 – 9.692)	0.026	1.116 (0.432 – 2.881)	0.821	1.412 (0.474 – 4.204)	0.535
PD-PD		2.469 (1.100 – 5.543)	0.028	3.063 (1.125 – 8.345)	0.026	4.109 (1.725 – 9.788)	0.001	5.461 (1.857 – 16.061)	0.002
Sex	Male	1	0.298	NA	-	1	0.681	NA	-
	Female	0.736 (0.414 – 1.310)				1.143 (0.604 – 2.162)			
Primary malignancy	Lung	1	0.056*	1	0.216*	1	0.012*	1	0.305*

*overall p-value

statistical significance, $p < 0.05$

CI = confidence interval; GKS = gamma knife radiosurgery; HR = hazard ratio; NA = not included in the analysis; PD = progressive disease; PIV = prescription isodose volume; RN = radiation necrosis; TRIC = treatment-related image change; WBRT = whole-brain radiation therapy.

		Overall survival				Progression-free survival			
	Breast	1.296 (0.610 – 2.753)	0.500	0.940 (0.427 – 2.071)	0.878	2.809 (1.317 – 5.990)	0.008	1.987 (0.830 – 4.760)	0.123
	Other	2.305 (1.165 – 4.559)	0.017	1.874 (0.866 – 4.055)	0.111	2.292 (1.050 – 5.002)	0.037	1.286 (0.535 – 3.090)	0.574
Prior GKS	No	1	0.300	1	0.548	1	0.938	1	0.900
	Yes	0.715 (0.379 – 1.379)		0.796 (0.378 – 1.676)		0.974 (0.504 – 1.883)		1.060 (0.431 – 2.607)	
WBRT	No	1	0.736	NA	-	1	0.272	NA	-
	Yes	0.890 (0.453 – 1.751)				0.633 (0.280 – 1.431)			
Primary malignancy control	Controlled	1	0.016	1	0.130	1	0.269	NA	-
	Uncontrolled	2.027 (1.143 – 3.595)		1.743 (0.849 – 3.579)		1.420 (0.762 – 2.647)			
*overall p-value									
statistical significance, $p < 0.05$									
CI = confidence interval; GKS = gamma knife radiosurgery; HR = hazard ratio; NA = not included in the analysis; PD = progressive disease; PIV = prescription isodose volume; RN = radiation necrosis; TRIC = treatment-related image change; WBRT = whole-brain radiation therapy.									

No major intraoperative complications were observed. One patient had newly developed hemiplegia in the immediate postoperative status, a predictable complication due to the location of the tumor in the thalamus.

Survival analysis

The median OS for the 86 patients was 21.7 months (95% confidence interval [CI]: 12.9–30.6 months). Kaplan-Meier estimates and median OS of each group are shown in Fig. 2. TRIC-RN patients displayed a tendency toward longer survival than patients of the pathologic PD group: 1-year and 2-year actuarial survival was 82.4% and 75.5% in the TRIC-RN group, respectively, compared to 63.2% and 41.5% in the TRIC-PD and 72.9% and 27.5% in the PD-PD group, respectively, although statistical significance was not observed ($p = 0.067$).

Forty-one patients (47%) exhibited progression of the resected lesion. Local recurrence was confirmed using diagnostic MRI in 7 (36%), 11 (47%), and 23 (71%) patients of the TRIC-RN, TRIC-PD, and PD-PD groups, respectively. The median PFS was obtained only for the PD-PD group (5.4 months [95% CI: 2.7–8.0 months]). There was a significant difference in PFS among the three groups (Fig. 3, $p < 0.0001$). In the post hoc test, the PD-PD

group exhibited a shorter time to progression than the other two groups (p = 0.001 vs. TRIC-RN and p = 0.002 vs. TRIC-PD), whereas no difference was observed between the TRIC-RN and TRIC-PD groups (p = 1.0) (Fig. 3).

Prognostic factors for survival and disease progression

In the univariate and multivariate analyses, a significant association was observed between the radio-surgical pathologic group and lesion progression (p = 0.0002 and p = 0.0016 in the univariate and multivariate analyses, respectively); there was a higher risk of recurrence in the PD-PD group, with a hazard ratio (HR) of 4.11 (95% CI: 1.73–9.79, p = 0.0002) in the univariate analysis and HR of 5.46 (95% CI: 1.86–16.06, p = 0.002) in the multivariate analysis, compared to that in the TRIC-RN group (HR = 1, reference). The risk of progression was not significantly different between the TRIC-RN and TRIC-PD groups (p = 0.535) (Table 2).

Uncontrolled primary malignancy was associated with a significantly higher risk of death than controlled primary malignancy only in the univariate analysis (HR: 2.027 [95% CI: 1.143–3.595], p = 0.020), and not in the multivariate analysis (p = 0.13). Primary malignancy showed a trend toward a higher risk of death in the univariate analysis (p = 0.056). The other cancer groups exhibited an HR of 2.305 (95% CI: 1.165–4.559, p = 0.02) compared to the lung cancer group, but no significant association in the multivariate analysis (p = 0.22). A higher prescription isodose (Gy) was associated with a significantly decreased risk of local progression only in the univariate analysis (HR: 0.887 [95% CI 0.796–0.989], p = 0.030) but not in the multivariate analysis (p = 0.25). For primary malignancy, breast cancer and other types of cancer exhibited higher risk of tumor recurrence than lung cancer in univariate analyses (overall p = 0.012, HR 2.809 [95% CI 1.317–5.990], p = 0.008 and HR 2.292 [95% CI 1.050–1.883], p = 0.037, respectively).

Illustrative case

A 73-year-old male patient with non-small cell lung cancer was diagnosed with a 2.9-cm brain metastatic lesion in the left temporo-occipital junction (Fig. 4, A). GKS with an initial prescription dose of 20 Gy at 50% isodose line (IDL) was performed. Due to suspicion of tumor progression at 11 months after the first session, a secondary prescription dose of 17 Gy at 50% IDL was administered (Fig. 4, B, IDL of the second GKS [yellow] and the previous session [blue]). After 9 months from the last GKS, the patient visited the emergency room with IICP signs, and MRI showed a lesion suspicious of TRIC with no distinct increase in CBV and absence of restricted diffusion (Fig. 4, C-E). Surgical resection was conducted, and the IICP improved. The pathology was confirmed as a mixture of tumor cells and RN (Fig. 5). Without adjuvant local therapy for the resected lesion, the patient was free of local progression for 15 months (Fig. 4, F).

Discussion

In this study, we investigated the clinical implications of TRIC-PD representing patients with discrepant radiopathology and surgical histopathology. Metastatic lesions featured as TRICs may worsen the neurological deficits and increase the frequency and cost of imaging to differentiate them from tumor progression[16–18].

A recent meta-analysis by Chuang et al.[14] investigated perfusion-weighted imaging (PWI) and magnetic resonance spectroscopy (MRS) for differentiating recurrent tumors from necrosis in patients with various brain tumors. Of the 397 patients in 13 studies, 95 patients had BM. The meta-analysis revealed that the relative CBV

derived from PWI, as well as MRS metabolite ratios in contrast-enhancing lesions, were significantly different in local progression compared to lesions resulting from radiation-related changes. Previous studies also reported variable diagnostic performance of PWI in sensitivity (range: 56–100%), specificity (range: 68–100%), and relative CBV threshold (range: 1.52–2.14) [13, 19, 20].

MRS appears to provide high specificity for detecting tumor recurrence (almost 100%). However, the relatively low sensitivity (range: 33–50%) and limited application for small-sized lesions (< 2 cm^3) are its two major drawbacks[13, 21]. The potential benefit of amino acid PET for differentiating pseudoprogression or RN from true disease progression following checkpoint inhibitor treatment of BM has been suggested, although the evidence is preliminary[22].

In our study, most TRIC or PD lesions, which worsened neurological deficits, were usually of large sizes with median volume of 6.41 cm^3 (range: 0.14–62.29 cm^3). Thus, we primarily utilized only PWI plus standard MRI protocols for the preoperative imaging to achieve the diagnostic accuracy and time-cost benefit in terms of determining urgent surgical resection.

With regard to clinical characteristics and prognosis, TRIC-PD group was compared to TRIC-RN or PD-PD groups. The patients in the TRIC-PD group had a larger PIV (median 9.40 cm^3) than patients in the TRIC-RN group (median 4.06 cm^3), with no differences in the median prescription dose of 18 Gy (range: 14–25 Gy in TRIC-RN and 8–22 Gy in TRIC-PD). When deriving the median diameter from the median PIV in our study, the median target size values of TRIC-RN and TRIC-PD were 15.95 mm and 21.1 mm, respectively. For targets in this range, a marginal dose of 21–24 Gy, or at least more than 18 Gy, has been suggested for local control according to previous studies[23–25]. Additionally, Amsbaugh et al.[26] demonstrated that a unit increase in the maximum dose (Gy) per target size (mm) was associated with a decreased local failure in SRS for BM, with the requirement for a higher prescription dose being proportional to the target size. This may explain the histologic local failure of TRIC-PD compared to TRIC-RN under the same marginal dose.

The TRIC-PD group exhibited a shorter time (median: 4.07 months) than the PD-PD group (median 8.77 months) from the last GKS session to the preoperative imaging diagnosis. Recent studies reported a local control rate in small-to-medium (1–3 cm)-sized BM lesions treated with 18 Gy of 87–93% at 6 months and 49–91% at 12 months.[16, 26] According to our results, some cases of early histologic local progression may have been overlooked due to the radiographic RN diagnosis. This would lead to a lower 6-month local control rate.

According to our survival analysis, the TRIC-RN group seems to have a better OS than the TRIC-PD and PD-PD groups, although statistical significance was not observed. For the risk of tumor recurrence after surgical resection, only the PD-PD group was significantly higher than other two groups in both the univariate and multivariate analyses. These results suggest a relatively benign prognosis of the TRIC-PD group compared to that of the PD-PD group, regardless of the same histologic tumor progression. Rather it shows a benign prognosis as the “pure RN” (TRIC-RN group), especially in aspect of local recurrence.

This study has several limitations. It is a retrospective single-center study with a small cohort. Further radiomics-oriented analysis is required for a more precise differentiation of TRICs and PD based on MR images, in terms of clinical prognosis. We did not include systemic therapies such as chemotherapy and immunotherapy, one of the possible risk factors for RN, due to the heterogeneity of individual therapeutic regimens.

In conclusion, notable histologic heterogeneity of metastatic lesions with TRICs after radiosurgery was observed, represented as the TRIC-PD group in this study. TRICs may be pure RN or more frequently mixed pathology of necrosis and viable tumor tissue. The postoperative clinical prognosis of patients with TRIC-PD was similar to that of the TRIC-RN group, and more indolent than that of the PD-PD group. These findings suggest that the imaging diagnosis of TRICs in advanced MRI may serve as a prognostic factor, regardless of their histologic heterogeneity.

Declarations

Funding:

Not applicable.

Conflicts of interest/Competing interests:

The authors report no conflict of interest concerning the materials or methods used in this study or the findings specified in this paper.

Availability of data and material:

The datasets used and/or analyzed during the current study are available from the corresponding author on reasonable request.

Code availability:

Not applicable.

Ethics approval:

Approval was obtained from the Samsung Medical Center Institutional Review Board.

Consent to participate/Consent for publication:

Consent was waived due to the retrospective nature of this study. All patient records were de-identified.

Author Contributions

Conception and design: Kim, Choi, Lee

Acquisition of data: Kim, Choi, Kong, Seol, Nam, Lee

Analysis and interpretation of data: Kim, Lee

Drafting the article: Kim,

Critically revising the article: Lee

Reviewed submitted version of manuscript: all authors

Approved the final version of the manuscript on behalf of all authors: Lee

Statistical analysis: Kim, Choi, Lee

Study supervision: Lee, Choi, Kong, Seol, Nam

References

1. Chao, S.T., et al., Challenges with the diagnosis and treatment of cerebral radiation necrosis. Int J Radiat Oncol Biol Phys, 2013. **87**(3): p. 449-57. https://doi.org/10.1016/j.ijrobp.2013.05.015
2. Kano, H., et al., The results of resection after stereotactic radiosurgery for brain metastases. Journal of neurosurgery, 2009. **111**(4): p. 825-831. https://doi.org/10.3171/2009.4.jns09246
3. Chin, L.S., L. Ma, and S. DiBiase, Radiation necrosis following gamma knife surgery: a case-controlled comparison of treatment parameters and long-term clinical follow up. Journal of neurosurgery, 2001. **94**(6): p. 899-904. https://doi.org/10.3171/jns.2001.94.6.0899
4. Gerosa, M., et al., Gamma knife radiosurgery for brain metastases: a primary therapeutic option. J Neurosurg, 2002. **97**(5 Suppl): p. 515-524. https://doi.org/10.3171/jns.2002.97.supplement
5. Petrovich, Z., et al., Survival and pattern of failure in brain metastasis treated with stereotactic gamma knife radiosurgery. J Neurosurg, 2002. **97**(5 Suppl): p. 499-506. https://doi.org/10.3171/jns.2002.97.supplement
6. Truong, M.T., et al., Results of surgical resection for progression of brain metastases previously treated by gamma knife radiosurgery. Neurosurgery, 2006. **59**(1): p. 86-97; discussion 86-97. https://doi.org/10.1227/01.neu.0000219858.80351.38
7. Chao, S., et al., Challenges with the diagnosis and treatment of cerebral radiation necrosis. Int J Radiat Oncol Biol Phys, 2013. **87**: p. 449-457. https://doi.org/10.1016/j.ijrobp.2013.05.015
8. Artzi, M., et al., Differentiation between treatment-related changes and progressive disease in patients with high grade brain tumors using support vector machine classification based on DCE MRI. Journal of Neuro-Oncology, 2016. **127**(3): p. 515-524. https://doi.org/10.1007/s11060-016-2055-7
9. Galldiks, N., et al., Imaging challenges of immunotherapy and targeted therapy in patients with brain metastases: response, progression, and pseudoprogression. Neuro Oncol, 2020. **22**(1): p. 17-30. https://doi.org/10.1093/neuonc/noz147
10. Walker, A.J., et al., Postradiation imaging changes in the CNS: how can we differentiate between treatment effect and disease progression? Future Oncol, 2014. **10**(7): p. 1277-97. https://doi.org/10.2217/fon.13.271
11. Cho, K.R., et al., Outcome of gamma knife radiosurgery for metastatic brain tumors derived from non-small cell lung cancer. J Neurooncol, 2015. **125**(2): p. 331-8. https://doi.org/10.1007/s11060-015-1915-x
12. Jeon, C., et al., Outcome of three-fraction gamma knife radiosurgery for brain metastases according to fractionation scheme: preliminary results. Journal of Neuro-Oncology, 2019. **145**(1): p. 65-74. https://doi.org/10.1007/s11060-019-03267-z
13. Huang, J., et al., Differentiation between intra-axial metastatic tumor progression and radiation injury following fractionated radiation therapy or stereotactic radiosurgery using MR spectroscopy, perfusion MR imaging or

volume progression modeling. Magnetic resonance imaging, 2011. **29**(7): p. 993-1001. https://doi.org/10.1016/j.mri.2011.04.004

14. Chuang, M.T., et al., Differentiating Radiation-Induced Necrosis from Recurrent Brain Tumor Using MR Perfusion and Spectroscopy: A Meta-Analysis. PLoS One, 2016. **11**(1): p. e0141438. https://doi.org/10.1371/journal.pone.0141438
15. Kerkhof, M., et al., Clinical applicability of and changes in perfusion MR imaging in brain metastases after stereotactic radiotherapy. Journal of neuro-oncology, 2018. **138**(1): p. 133-139. https://doi.org/10.1007/s11060-018-2779-7
16. Vogelbaum, M.A., et al., Local control of brain metastases by stereotactic radiosurgery in relation to dose to the tumor margin. Journal of neurosurgery, 2006. **104**(6): p. 907-912. https://doi.org/10.3171/jns.2006.104.6.907
17. McKay, W.H., et al., Repeat stereotactic radiosurgery as salvage therapy for locally recurrent brain metastases previously treated with radiosurgery. Journal of neurosurgery, 2016. **127**(1): p. 148-156. https://doi.org/10.3171/2016.5.jns153051
18. Minniti, G., et al., Multidose stereotactic radiosurgery (9 Gy × 3) of the postoperative resection cavity for treatment of large brain metastases. Int J Radiat Oncol Biol Phys, 2013. **86**(4): p. 623-9. https://doi.org/10.1016/j.ijrobp.2013.03.037
19. Hatzoglou, V., et al., A prospective trial of dynamic contrast-enhanced MRI perfusion and fluorine-18 FDG PET-CT in differentiating brain tumor progression from radiation injury after cranial irradiation. Neuro-oncology, 2016. **18**(6): p. 873-880. https://doi.org/10.1093/neuonc/nov301
20. Mitsuya, K., et al., Perfusion weighted magnetic resonance imaging to distinguish the recurrence of metastatic brain tumors from radiation necrosis after stereotactic radiosurgery. Journal of neuro-oncology, 2010. **99**(1): p. 81-88. https://doi.org/10.1007/s11060-009-0106-z
21. Chernov, M.F., et al., Multivoxel proton MRS for differentiation of radiation-induced necrosis and tumor recurrence after gamma knife radiosurgery for brain metastases. Brain tumor pathology, 2006. **23**(1): p. 19-27. https://doi.org/10.1007/s10014-006-0194-9
22. Galldiks, N., et al., PET imaging in patients with brain metastasis-report of the RANO/PET group. Neuro Oncol, 2019. **21**(5): p. 585-595. https://doi.org/10.1093/neuonc/noz003
23. Mohammadi, A.M., et al., Impact of the radiosurgery prescription dose on the local control of small (2 cm or smaller) brain metastases. Journal of Neurosurgery, 2017. **126**(3): p. 735-743. https://doi.org/10.3171/2016.3.jns153014
24. Wiggenraad, R., et al., Dose–effect relation in stereotactic radiotherapy for brain metastases. A systematic review. Radiotherapy and Oncology, 2011. **98**(3): p. 292-297. https://doi.org/10.1016/j.radonc.2011.01.011
25. Lippitz, B., et al., Stereotactic radiosurgery in the treatment of brain metastases: the current evidence. Cancer treatment reviews, 2014. **40**(1): p. 48-59. https://doi.org/10.1016/j.ctrv.2013.05.002
26. Amsbaugh, M., et al., Dose-volume response relationship for brain metastases treated with frameless single-fraction linear accelerator-based stereotactic radiosurgery. Cureus, 2016. **8**(4). https://doi.org/10.7759/cureus.587

Figures

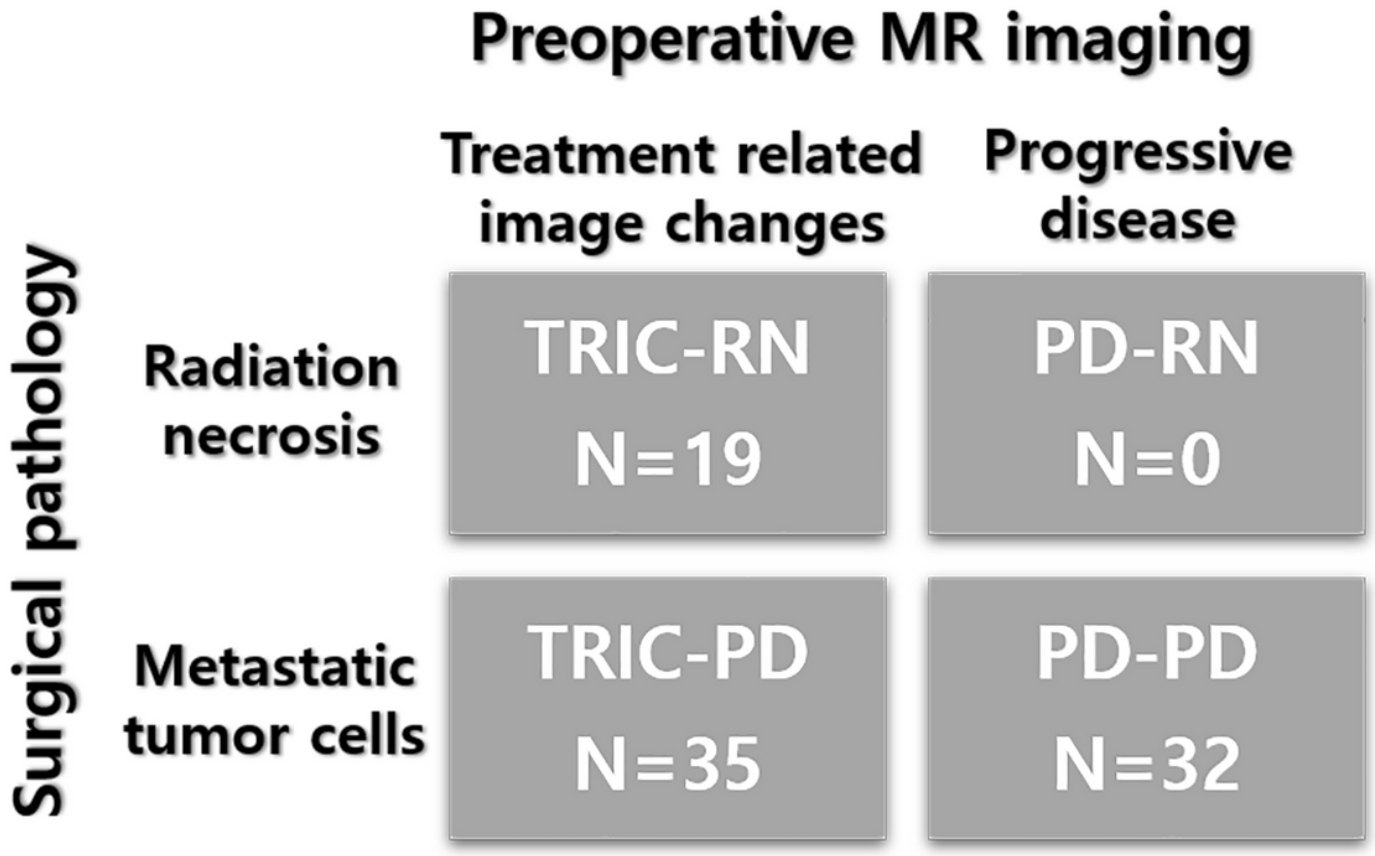

Figure 1

Patient classification. A total of 86 patients were initially classified into four groups according to preoperative MRI and surgical pathology. For surgical pathology, only pure radiation necrosis was sorted into “radiation necrosis.” Mixed pathology, containing both metastatic tumor and necrotic cells, was classified as “metastatic cells.” No patient was assigned to the PD-RN group; therefore, the three groups TRIC-RN, TRIC-PD, and PD-PD were finally included in the present study MRI = magnetic resonance imaging; PD = progressive disease; RN = radiation necrosis; TRIC = treatment-related image change

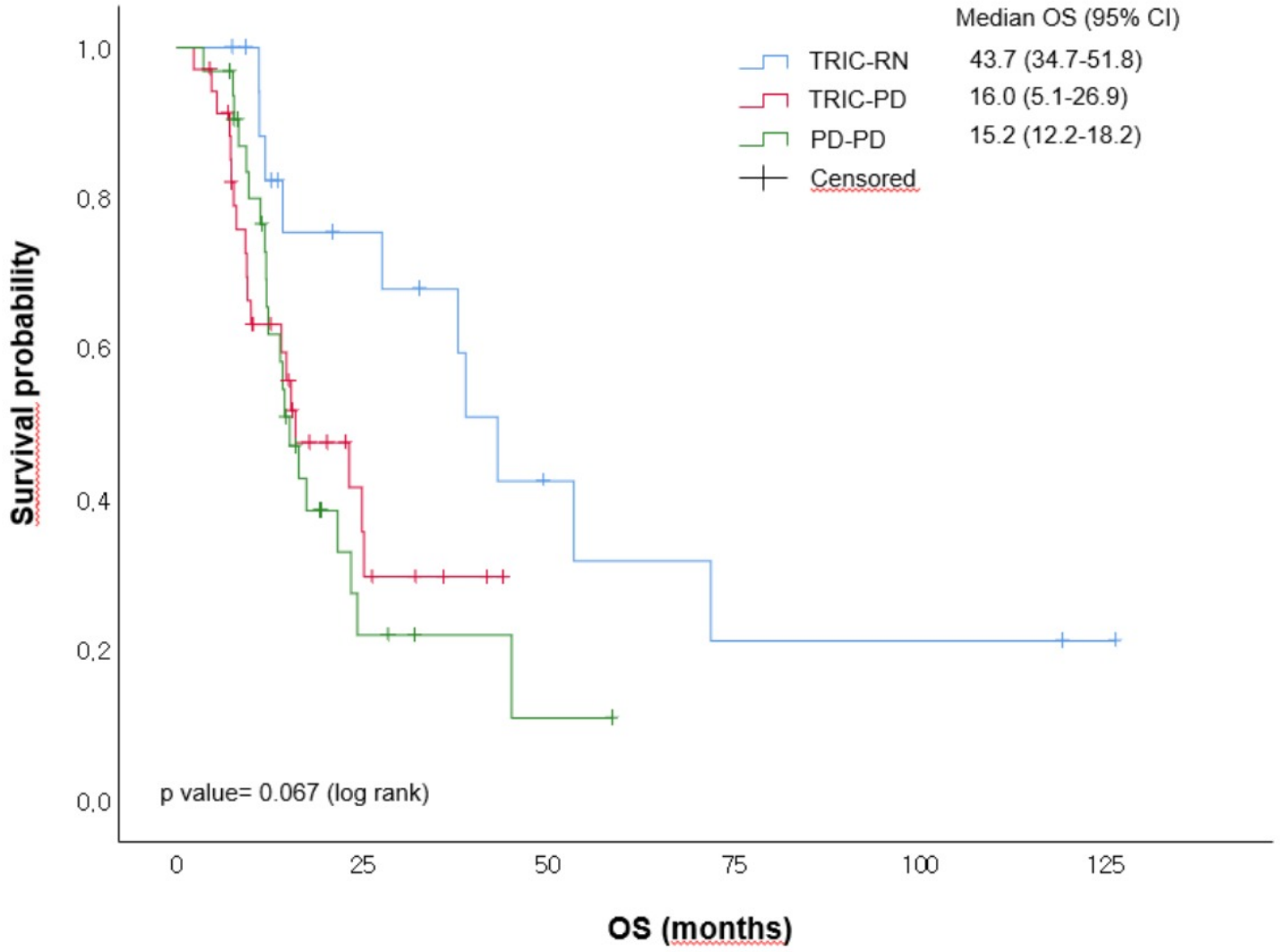

Figure 2

Kaplan-Meier estimate of overall survival

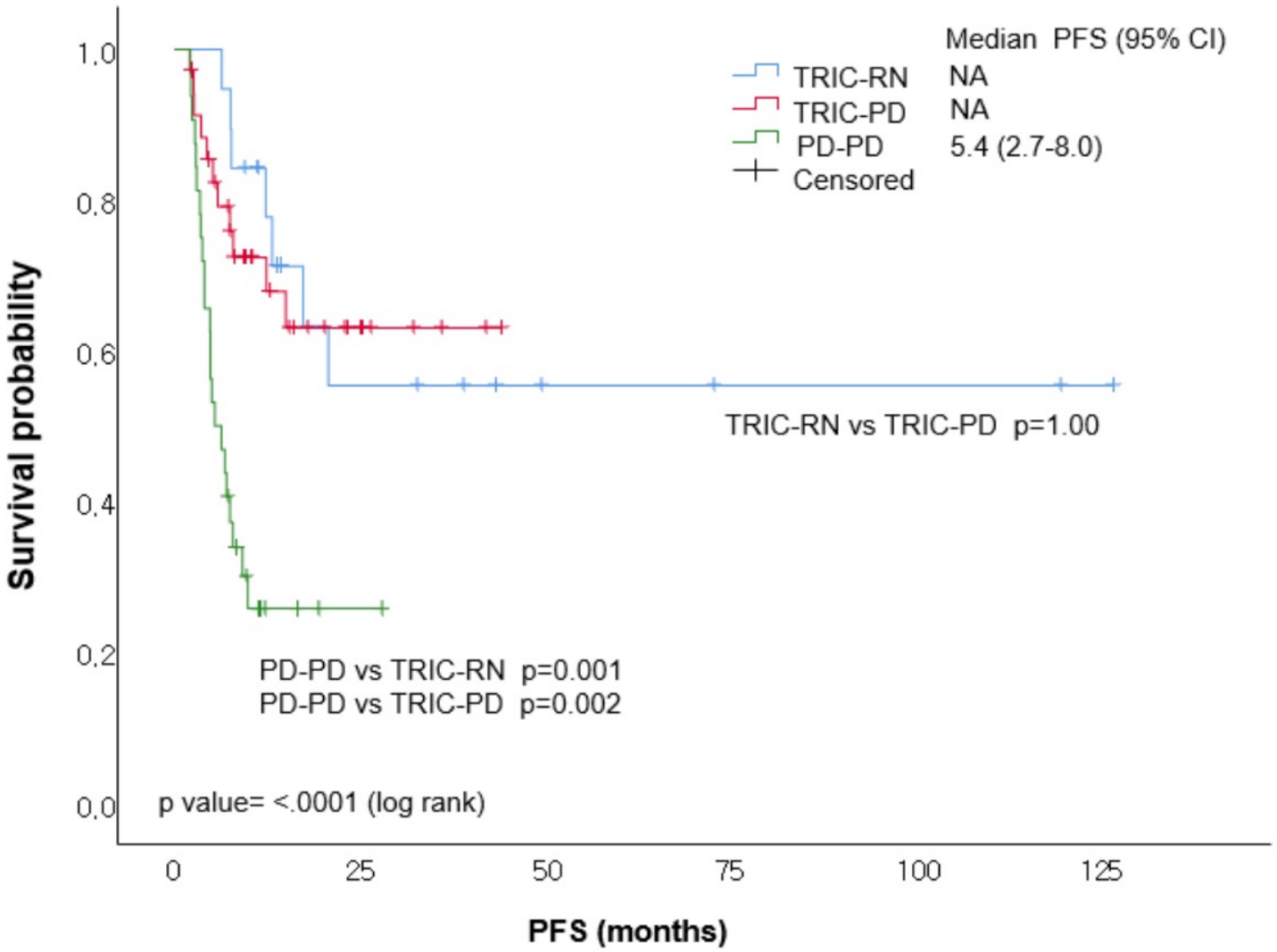

Figure 3

Kaplan-Meier estimate of progression-free survival

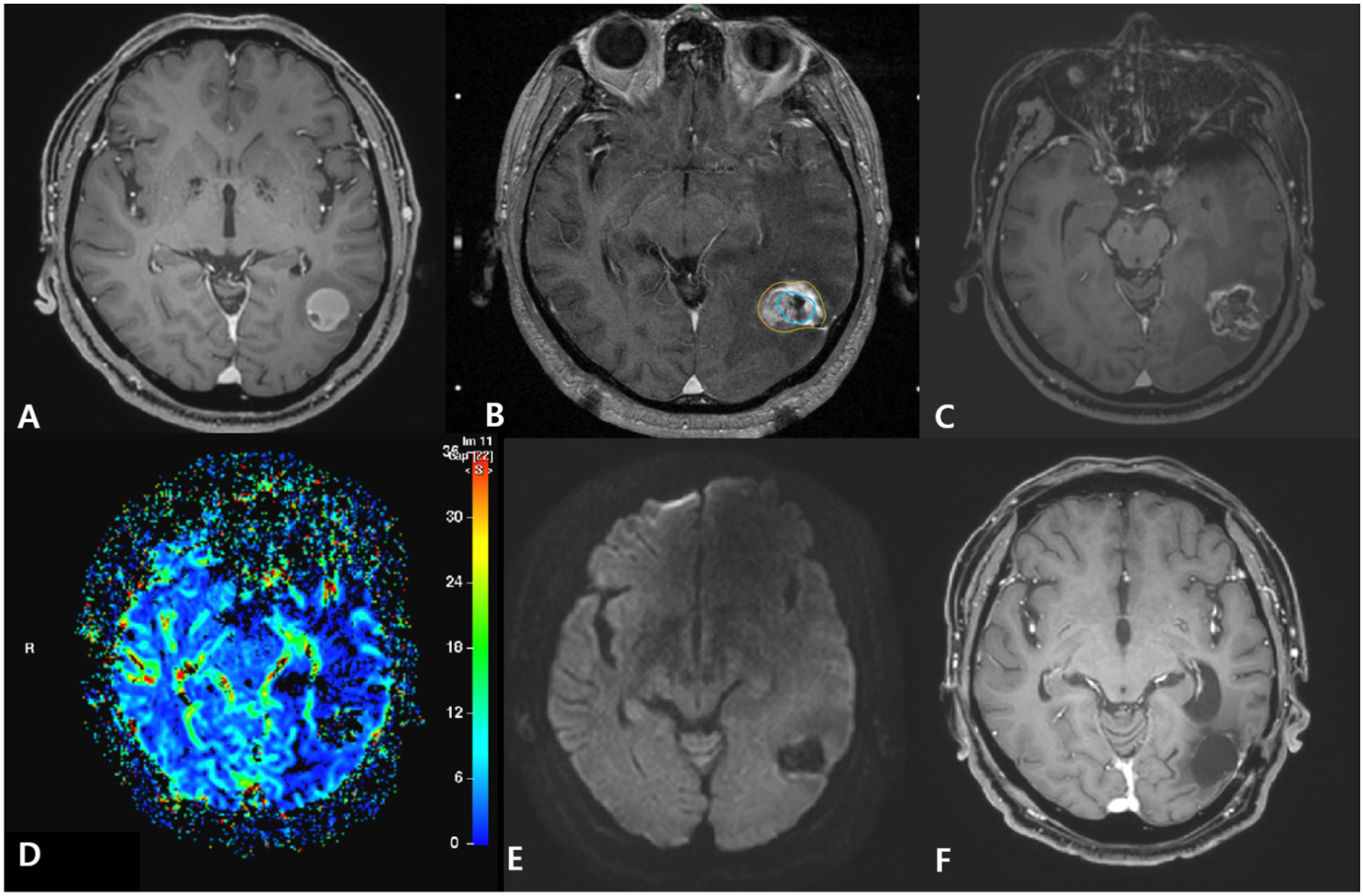

Figure 4

An illustrative case of TRIC-PD

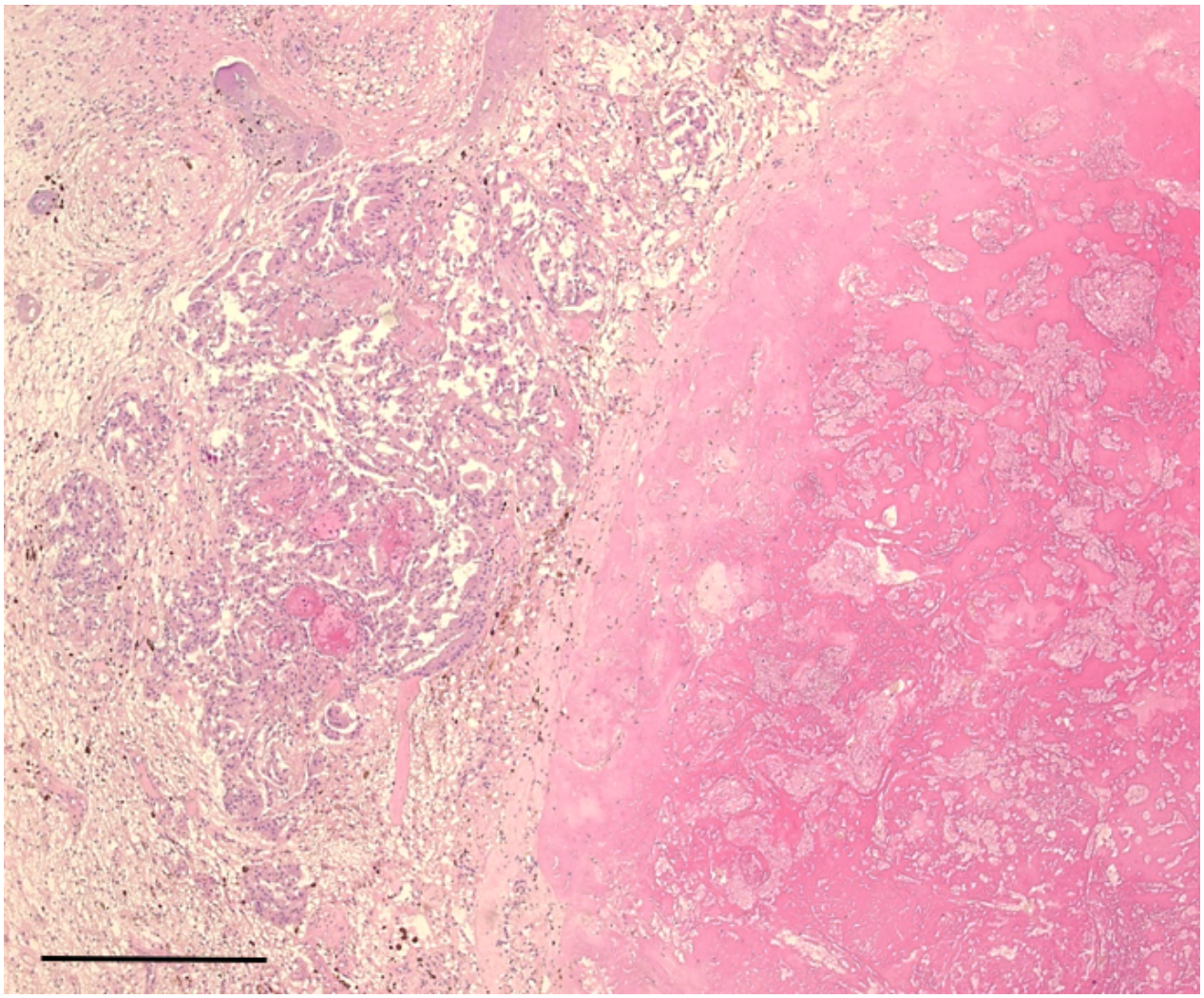

Figure 5

Representative histopathologic features of TRIC-PD. Adjacent to a large, confluent necrotic portion (Right), an area with viable tumor cells (Left) was present, rendering a diagnosis of metastatic adenocarcinoma. (hematoxylin and eosin stain, x100, scale bar=500 μm)